JOURNAL OF VIROLOGY, Apr. 2001, p. 3343–3351 Vol. 75, No. 7
0022-538X/01/$04.00+0 DOI: 10.1128/JVI.75.7.3343–3351.2001

Roles of Macrophages in Measles Virus Infection of Genetically Modified Mice

BRANKA ROSCIC-MRKIC,[1] RETO A. SCHWENDENER,[2] BERNHARD ODERMATT,[3] ARMANDO ZUNIGA,[1] JOVAN PAVLOVIC,[4] MARTIN A. BILLETER,[1] AND ROBERTO CATTANEO[5]*

Molecular Biology Institute,[1] Pathology Institute,[3] and Medical Virology Institute,[4] University of Zurich, Zurich, and Laboratory of Liposome Research, Medical Radiobiology, Paul Scherrer Institute, Villigen,[2] Switzerland, and Molecular Medicine Program, Mayo Clinic, Rochester, Minnesota[5]

Received 13 November 2000/Accepted 3 January 2001

Knowledge of the mechanisms of virus dissemination in acute measles is cursory, but cells of the monocyte/macrophage (MM) lineage appear to be early targets. We characterized the dissemination of the Edmonston B vaccine strain of measles virus (MV-Ed) in peripheral blood mononuclear cells (PBMC) of two mouse strains expressing the human MV-Ed receptor CD46 with human-like tissue specificity and efficiency. In one strain the alpha/beta interferon receptor is defective, allowing for efficient MV-Ed systemic spread. In both mouse strains the PBMC most efficiently infected were F4/80-positive MMs, regardless of the inoculation route used. Circulating B lymphocytes and CD4-positive T lymphocytes were infected at lower levels, but no infected CD8-positive T lymphocytes were detected. To elucidate the roles of MMs in infection, we depleted these cells by clodronate liposome treatment in vivo. MV-Ed infection of splenic MM-depleted mice caused strong activation and infection of splenic dendritic cells (DC), followed by enhanced virus replication in the spleen. Similarly, depletion of lung macrophages resulted in strong activation and infection of lung DC. Thus, in MV infections of genetically modified mice, blood monocytes and tissue macrophages provide functions beneficial for both the virus and the host: they support virus replication early after infection, but they also contribute to protecting other immune cells from infection. Human MM may have similar roles in acute measles.

Measles virus (MV) causes a highly contagious disease that is a major cause of childhood morbidity and mortality in developing countries. After person-to-person transmission by the respiratory route, the virus spreads from the upper respiratory tract mucosa and lungs to lymphoid tissues, where replication occurs primarily in macrophage- and lymphoid-multinucleated giant cells (37, 38, 43). MV also spreads to numerous other organs, and in these the virus replicates in endothelial and epithelial cells (26). The rash occurring about 2 weeks after infection marks the onset of a strong immune response which is effective in clearing virus and establishing long-term immunity (13). However, at this time numerous abnormalities of immune responses are also detected, which contribute to measles morbidity and mortality (5). This immune suppression is milder after vaccination with the live attenuated strain Edmonston B (MV-Ed).

Characterization of the first steps in systemic MV dissemination is a priority because it may give insights into mechanisms of MV pathogenesis, including immune suppression. Since humans are the only natural MV host, and human tissues can rarely be obtained immediately after contagion, knowledge of the first steps in systemic MV dissemination is at best cursory. Nevertheless, MV infection has been detected in several types of human peripheral blood mononuclear cells (PBMC), including monocytes (8, 17, 20), but also T and B lymphocytes (29). Moreover, dendritic cells (DC) can be infected in vitro (11, 14, 34). In cases where the virus disseminates in the central nervous system (13), CD68-positive hematogenous macrophages/microglia cells are infected (25).

In the absence of a small-animal model that mimics human disease, information about the initial steps of MV dissemination has been initially sought in primates. Experimentally infected monkeys develop a disease similar to that of humans (24), and PBMC become positive for MV as early as 2 days postinfection (p.i.), with a peak on day 7 (1, 32, 45). Histological examinations of monkey lymphoid tissues revealed prominent infection of both macrophage- and lymphoid-multinucleated giant cells (15, 24, 36) similar to those found in humans.

Ethical considerations and the fact that primates are costly and in short supply have driven the development of rodent models for MV infection. Genetically modified mice expressing a human MV receptor have recently been produced with the intent of establishing a practical animal model of measles. In particular, mice expressing the ubiquitous regulator of complement activation CD46, one of the MV receptors (7, 30, 39) with human-like tissue specificity, were developed (4, 28, 44). Notwithstanding that in two of these mouse strains lung MV replication was below (4) or only slightly above (28) the detection level, in a third mouse strain MV replication in PBMC and lymphoid tissues was clearly documented (31). These MV infection-permissive mice express CD46 at levels higher than those in humans (21), possibly because they have multiple integrated copies of the CD46 gene (44). Moreover, after crossing one of these mouse strains in an alpha/beta interferon receptor knockout background, efficient MV replication in lungs and lymphatic organs was documented (27, 28). Based on the observation that in infected organs virus replication was

* Corresponding author. Mailing address: Molecular Medicine Program, Mayo Clinic, Guggenheim 18, 200 First St. SW, Rochester, MN 55905. Phone: (507) 284 0171. Fax: (507) 266 2122. E-mail: cattaneo.roberto@mayo.edu.

often monitored in F4/80-positive cells, macrophages were identified as potential vectors for MV dissemination in mice (27). Consistent with this observation, monocytes/macrophages (MM), which serve generally as a first-line defense in the innate immune system against pathogens (9), appear to be prime target cells for MV during acute infection in humans (8).

In this study, we aimed at characterizing the host cells replicating MV immediately after infection. We used our two mouse strains expressing CD46 with human-like tissue specificity and efficiency, one (CD46Ge) with a functional alpha/beta interferon receptor, the other (Ifnar^{ko}-CD46Ge) lacking this receptor. The levels of infection of different classes of PBMC were quantified; F4/80-positive (F4/80^{+}) MM were infected with the highest efficiency in both mouse strains. Systemic MV spread was then monitored in Ifnar^{ko}-CD46Ge mice. When MM were depleted by clodronate liposomes treatment in vivo, numerous infected DC were detected in the spleen and lungs, and splenic virus replication was increased.

MATERIALS AND METHODS

Animals and infections. The two genetically modified mouse lines, CD46Ge, expressing a human CD46 gene with human-like tissue specificity, and Ifnar^{ko}-CD46Ge, with in addition a defective (knockout insertion) alpha/beta interferon receptor gene, have been described previously (28).

Animals were bred under specific-pathogen-free conditions and infected at 5 to 8 weeks of age. Infection of anesthetized mice was performed intranasally (i.n.) with 10^6 PFU of MV-Ed in 50 μl, intraperitoneally (i.p.) in 200 μl, or intracerebrally (i.c.) in 30 μl. Noninfected or mock-infected mice inoculated with the postnuclear fraction of uninfected Vero cells served as controls.

Viruses. Tagged MV-Ed vaccine virus was used (33). All virus stocks were propagated in Vero cells and quantified by standard plaque assay on Vero cells.

Flow cytometric analysis on PBMC. Blood samples were collected from infected animals, and PBMC were isolated by gradient centrifugation on Ficoll-Paque (Pharmacia, Uppsala, Sweden) for 30 min at 400 × *g*. Isolated mouse PBMC were washed three times with phosphate-buffered saline (PBS) containing 2% fetal calf serum (FCS) and then resuspended at a density of 10^6 cells/200 μl. A double-staining assay, i.e., MV versus cell type-specific staining, was performed by incubating PBMC with biotinylated anti-MV H monoclonal antibody clone 55 (1:100) (kindly provided by Branka Horvat and Fabian Wild, Lyon, France) and appropriate cell-specific antibodies (1 μg per million cells) for 60 min on ice. The following cell-specific rat anti-mouse antibodies were used: for identification of CD4 T cells, fluorescein isothiocyanate (FITC)-conjugated anti-CD4; for CD8 T cells, anti-CD8–FITC; for B cells, anti-CD45R/B220–FITC; and for F4/80 MM, anti F4/80–FITC. All antibodies were from Serotec, United Kingdom. After three washes with PBS containing 2% FCS, samples were incubated for a further 45 min with a streptavidin-phycoerythrin conjugate for labeling of biotinylated primary anti-MV antibodies (PharMingen, San Diego, Calif.) When Fc receptor-expressing cell populations (B lymphocytes or MM) were analyzed, the samples were preincubated with Fc Block (PharMingen) for 15 min on ice in order to reduce Fc receptor-mediated binding. The samples from noninfected mice served as negative controls, and MV-infected Vero cells served as a positive control. Flow cytometry analyses were carried out on a FACScan instrument (Becton Dickinson). A live gate based on forward and side scatter was used to exclude dead cells and doublets; at least 20,000 events were collected for T or B cells, and at least 10,000 events were collected for MM. A fixed window was set on the positive cell-specific population in order to count the number of MV-positive specific cells in PBMC bulk culture. Statistical analysis was done with CricketGraph 3.0 software after background correction, and means of numbers and percentages of double-stained positive cells are presented. It is of note that MV-induced syncytia are large size and have poor viability, and thus only MV-infected single cells could be analyzed with this method.

CD46 was detected on the surface of PBMC by incubation with anti-CD46 monoclonal antibody clone 11/88 (1:50, vol/vol) and labeling with goat anti-mouse immunoglobulin G1–R-phycoerythrin conjugate (Southern Biotechnology Associates, Birmingham, Ala.).

Reisolation of MV from PBMC. Heparinized blood specimens were collected from infected mice on day 3 p.i., and PBMC were isolated as described above and washed five times with PBS containing 10% FCS and twice with Dulbecco's modified Eagle's medium supplemented with 10% FCS. Fractionation of cell populations was done by adherence to plastic in a 12-well tissue culture plate (Becton Dickinson) for 3 h at 37°C. After adsorption, the nonadherent cells were transferred to a new 12-well tissue culture plate at a density of 10^6 cells/ml, and the culture medium was supplemented with 10 U of mouse interleukin-2 (Sigma) per ml and 10 μg of lipopolysaccharide (LPS) (Sigma) per ml. The adherent cells were washed with PBS and then cultured in Dulbecco's modified Eagle's medium with 10% FCS, supplemented with 10 μg of LPS per ml. After 3 days of LPS-stimulation, Vero cells in suspension were added at a density of 10^4 cells/ml, and cultures were monitored for cytopathic changes during three passages. The presence of MV in cocultures was confirmed by reverse transcription (RT)-PCR as described below.

Preparation of clodronate liposomes. Clodronate liposomes were prepared as previously described (35). Briefly, liposomes composed of soy phosphatidylcholine, cholesterol and DL-α-tocopherol at 40 mg of soy phosphatidylcholine, 6 mg of cholesterol, and 0.2 mg of tocopherol per ml (1:0.3:0.01 mol parts) were prepared by freeze-thawing and filter extrusion. The dry lipid mixture was solubilized by addition of 1 ml of clodronate solution (Ostac; Boehringer Mannheim; 37.5 mg of sodium clodronate). The resulting multilamellar vesicles were freeze-thawed in three cycles of liquid nitrogen and water at 40°C, followed by repetitive (five times) filter extrusion through 400-nm-pore-size membranes (Nuclepore; Sterico, Dietikon, Switzerland) using a Lipex extruder (Lipex Biomembranes Inc., Vancouver, Canada). For the determination of clodronate encapsulation efficiency, the preparations were trace labeled with $^{45}CaCl_2$ (Amersham Pharmacia Biotech, Dübendorf, Switzerland) and 1 mM $CaCl_2$ as carrier. Unencapsulated clodronate was removed in two steps by concentration to 4 to 5 ml with an Amicon ultrafiltration cell using a YM100 (100-kDa cutoff) membrane followed by size exclusion chromatography on a Sephadex G25 column (30 by 2.5 cm; Pharmacia) with phosphate buffer (67 mM, pH 7.4) as the eluent. The diluted liposomes collected after column elution were reconcentrated by ultrafiltration to obtain a final volume of 3 to 4 ml containing 8 to 12 mg of clodronate/ml. All preparations were sterile filtered through a 0.45-μm-pore-sized filter (Gelman). Liposome size and homogeneity were routinely measured with a Nicomp (Santa Barbara, Calif.) 370 laser light-scattering particle sizer. The clodronate liposomes were used within 10 days after preparation.

Macrophage depletion in vivo. Depletion of splenic macrophages in 5- to 8-week-old mice was achieved by i.p. injection of 2 mg of clodronate liposomes per animal. Mice injected with the same volume of empty liposomes were used as a control. Three days later, mice were injected i.p. with 10^6 PFU of MV-Ed. Mouse specimens, including spleen, liver, lung, and blood, were harvested at 3 days after virus administration for analyses of MV pathogenesis. Macrophage depletion efficiency was monitored by cell-specific analysis of collected tissues and fluorescence-activated cell sorter analysis of F4/80-positive cells in the peripheral blood samples.

For depletion of lung-associated macrophages, 1 mg of clodronate liposomes per mouse was administered i.n. 3 days and 1 day before virus infection, and the lung tissues and blood samples were collected 3 days after i.n. administration of 10^6 PFU of MV-Ed.

MV RNA quantification by real-time PCR analysis. Total RNA from mouse organs was extracted as previously described (28). For RT, the minus-strand primer 5′-TTATAACAATGATGGAGGGTAGGC, hybridizing to the last 24 nucleotides of the N mRNA, was used. Real-time quantitative TaqMan PCR based on the primer pair 5′-GGGTACCATCCTAGCCCAAATT and 5′-CGA ATCAGCTGCCGTGTCT, amplifying 73 bases of the N mRNA, and the molecular beacon 5′-FAM-CGCAAAGGCGGTTACGGCCC-DABCYL, where 6-carboxyfluorescein (FAM) serves as the reporter fluorochrome and 4-dimethylaminophenylazobenzoic acid (DABCYL) serves as the quencher, was performed according to the protocol of the supplier (Perkin-Elmer, Applied Biosystems). Briefly, each 25-μl reaction mixture contained 2 μl of cDNA from the RT reaction, 12.5 μl of TaqMan PCR Master Mix (Perkin-Elmer), a 240 nM concentration of each primer, and 160 nM molecular beacon. One cycle of denaturation (95°C for 10 min) was applied, followed by 45 cycles of amplification (95°C for 15 s and 60°C for 1 min). PCR was carried out in a spectrophotometric thermal cycler (ABI PRISM 7700 Sequence Detection System; Perkin-Elmer) that monitors changes in the fluorescence spectrum of molecular beacon FAM in each reaction tube during the course of the reaction, resulting in a real-time analysis.

For real-time PCR quantification, a standard curve was generated from triplicate samples of purified MV N RNA transcribed in vitro. Briefly, an MV N gene-containing plasmid, p(+)MNPCAT (33), was linearized with *Stu*I and transcribed in vitro by using T7 RNA polymerase. After digestion of the DNA template with RNase-free DNase I (Roche, Basel, Switzerland), the generated

MV N RNA transcript was purified and analyzed on an agarose gel, followed by determination of the concentration by spectrophotometry. The linear copy number range from 4×10^{10} to 4×10^{3} copy equivalents per reaction (10-fold dilutions) was taken for RT-PCR amplification and detection of corresponding threshold cycles, which ranged from 14 to 31, corresponding to 4×10^{10} to 4×10^{3} MV N RNA copy equivalents per RT-PCR, respectively. The determined viral RNA load was expressed as MV N RNA copy number per 1 μg of total RNA, and the calculation of MV N RNA copies per average cell was done by considering that about 2×10^{5} splenic cells contain approximately 1 μg total RNA.

Histological, IHC, and ISH assays. Histological, immunohistochemistry (IHC) and in situ hybridization (ISH) assays were done as described previously (27). Briefly, mouse tissue specimens for IHC analysis were collected at the times indicated, immersed in Hanks balanced salt solution, and snap frozen in liquid nitrogen. Two- to three-micrometer-thick tissue sections were cut in a cryostat, fixed with acetone, and stored at −70°C. Specimens for ISH were fixed in 4% PBS-buffered formaldehyde, embedded in paraffin, and then cut at 2 μm.

For the staining of cell differentiation markers, the following primary rat anti-mouse monoclonal antibodies were used: antibodies against CD45R/B220 (RA3-6B2; PharMingen), CD3 (KT3), CD4 (YTS 191), CD8 (YTS 169), F4/80 macrophages (A3-1) (American Type Culture Collection, Manassas, Va.), splenic marginal metallophilic or marginal zone macrophages (MOMA1 or ERTR9) (Biomedicals AG, Augst, Switzerland), follicular DC (4C11), and interdigitating DC (NLDC145) (Biomedicals AG). CD11c was stained with a primary monoclonal hamster antibody (N418). Detection of newly formed germinal centers was done with anti-peanut agglutinin (anti-PNA) and polyclonal rabbit anti-PNA antibodies. Primary antibodies were revealed by sequential incubation with alkaline phosphatase-labeled species-specific secondary antibodies (Jackson ImmunoResearch Labs, West Grove, Pa.). Alkaline phosphatase was visualized using naphthol AS-BI (6-bromo-2-hydroxy-3-naphtholic acid-2-methoxy anilide) phosphate and new fuchsin (Sigma) as a substrate, yielding a red reaction product. Sections were counterstained with hemalum.

Detection of MV N mRNA in situ was performed with a digoxigenin-labeled N RNA probe on prehybridized paraffin sections under appropriate conditions as previously described (28). Hybridized probes were immunologically detected using a digoxigenin-nucleic acid detection kit (Roche).

RESULTS

MV replication in PBMC. MV-infected F4/80$^+$ macrophages were detected after i.n. inoculation in several tissues of Ifnar^{ko}-CD46Ge mice, raising the possibility that these cells may disseminate MV infection (27). Previous studies revealed that PBMC of these animals are MV positive (28) without establishing which subtypes of circulating PBMC are infected. To obtain this information, we analyzed MV H protein expression at the surface of B220$^+$ B cells, CD4$^+$ T cells, CD8$^+$ T cells, or F4/80$^+$ MM isolated from infected Ifnar^{ko}-CD46Ge mice and from the parental CD46Ge animals. Double-labeling flow cytometric analysis was performed 3 and 6 days after i.n. or i.p. infection with MV-Ed.

Three days after i.n. infection, most Ifnar^{ko}-CD46Ge mice (seven of nine animals) expressed the H protein on about 1.8% of F4/80$^+$ cells (Table 1). H antigen was also detected in a smaller fraction of B220$^+$ B lymphocytes and CD4$^+$ T cells in fewer animals. In contrast, H protein expression was not detectable on CD8$^+$ T cells.

Ifnar^{ko}-CD46Ge mice were then injected i.p. with the same amount of virus, and their PBMC were examined. As shown in Table 1, at 3 days p.i. H protein was observed at an average of 3.2% on F4/80$^+$ cells, and at 0.8 to 1% on B220$^+$ B cells or CD4$^+$ T cells, in the majority of animals. In contrast, CD8$^+$ T cells were weakly positive in only one of five mice. Thus, 3 days after either i.n. or i.p. inoculation of Ifnar^{ko}-CD46Ge mice, F4/80$^+$ MM were infected at levels that were about three times higher than those for B220$^+$ B cells or CD4$^+$ T cells; in contrast, infection of CD8$^+$ T cells was negligible.

TABLE 1. MV H protein expression in peripheral blood cells of Ifnar^{ko}-CD46Ge and CD46Ge mice inoculated i.n. or i.p. with MV-Ed

Cell type	No. of MV H protein-positive mice/total[a]		
	Ifnar^{ko}-CD46Ge		CD46Ge (i.p. inoculated)
	i.n. inoculated	i.p. inoculated	
F4/80$^+$	7/9 (1.81 ± 1.02)	4/5 (3.24 ± 1.86)	6/7 (1.37 ± 0.63)
B220$^+$	6/9 (0.58 ± 0.48)	3/5 (0.78 ± 0.44)	4/7 (0.67 ± 0.29)
CD4$^+$	4/9 (0.62 ± 0.46)	5/5 (0.99 ± 0.80)	6/7 (0.54 ± 0.28)
CD8$^+$	0/9	1/5 (0.67)	0/7

[a] In parentheses is the percentage of positive cells (mean ± standard deviation after background correction); only positive animals were considered. On average 1,300 F4/80$^+$ cells, 7,600 B220$^+$ cells, 4,100 CD4$^+$ T cells, and 2,000 CD8$^+$ T cells were counted. Fluorescence-activated cell sorter analysis of CD46 expression on cells of eight mice revealed a mean fluorescence of 24 for F4/80$^+$ cells, 30 for B220$^+$ cells, 11 for CD4$^+$ T cells, 5 for CD8$^+$ T cells, and 0.1 for erythrocytes.

MV infection of immune cells was also examined at 6 days p.i. in other groups of mice inoculated i.n. or i.p. with MV-Ed. At this later time the expression of H antigen on both MM and lymphatic cells was still positive, and preferential replication in F4/80$^+$ cells was confirmed (data not shown).

In addition, we investigated if the virus was recovered from adherent or nonadherent PBMC subsets isolated from i.p. infected Ifnar^{ko}-CD46Ge mice. Virus recovery was positive, after stimulation with LPS as a mitogen and cocultivation with Vero cells, in three of seven instances when adherent cells were used and in one case for the nonadherent cells.

We then asked if preferential MV replication in MM requires interferon receptor knockout as well as CD46 positivity. To this end, we infected the parental mouse line, CD46Ge, expressing human CD46 with human-like tissue specificity and having an intact interferon type I receptor, with the same virus. As shown in Table 1, at 3 days p.i. MV H expression was observed at about 1.4% of F4/80$^+$ cells of most i.p. infected mice and again at two- to three-times lower levels in lymphoid B220$^+$ B or CD4$^+$ T cells. CD8$^+$ T cells were negative. When PBMC of CD46Ge mice were analyzed at 6 days p.i., no positive cells were detected (data not shown). As a control, wild-type C57BL/6 mice were also infected with the same inoculum. No positive H protein staining was detected in the immune cells of these animals. We thus conclude that efficient MV infection of F4/80$^+$ MM depends on human CD46 expression in these cells.

Previously, we found that lymphocytes of CD46Ge mice express CD46 levels comparable to those of human lymphocytes (28), but we did not compare CD46 expression in different PBMC populations. We therefore performed this analysis and determined that B220$^+$ cells had the highest CD46 expression levels, followed by F4/80$^+$, CD4$^+$, and CD8$^+$ cells (mean fluorescence of 30, 24, 11, and 5, respectively, data not shown). We conclude that there is no direct correlation between the level of human CD46 expression and the efficiency of MV infection.

Different inoculation routes lead to efficient infection of F4/80$^+$ macrophages. As shown in Table 1, levels of MV infection in PBMC, including MM, are highest after i.p. inoculation. Since data on systemic MV replication in Ifnar^{ko}-CD46Ge mice were previously obtained only after i.n.

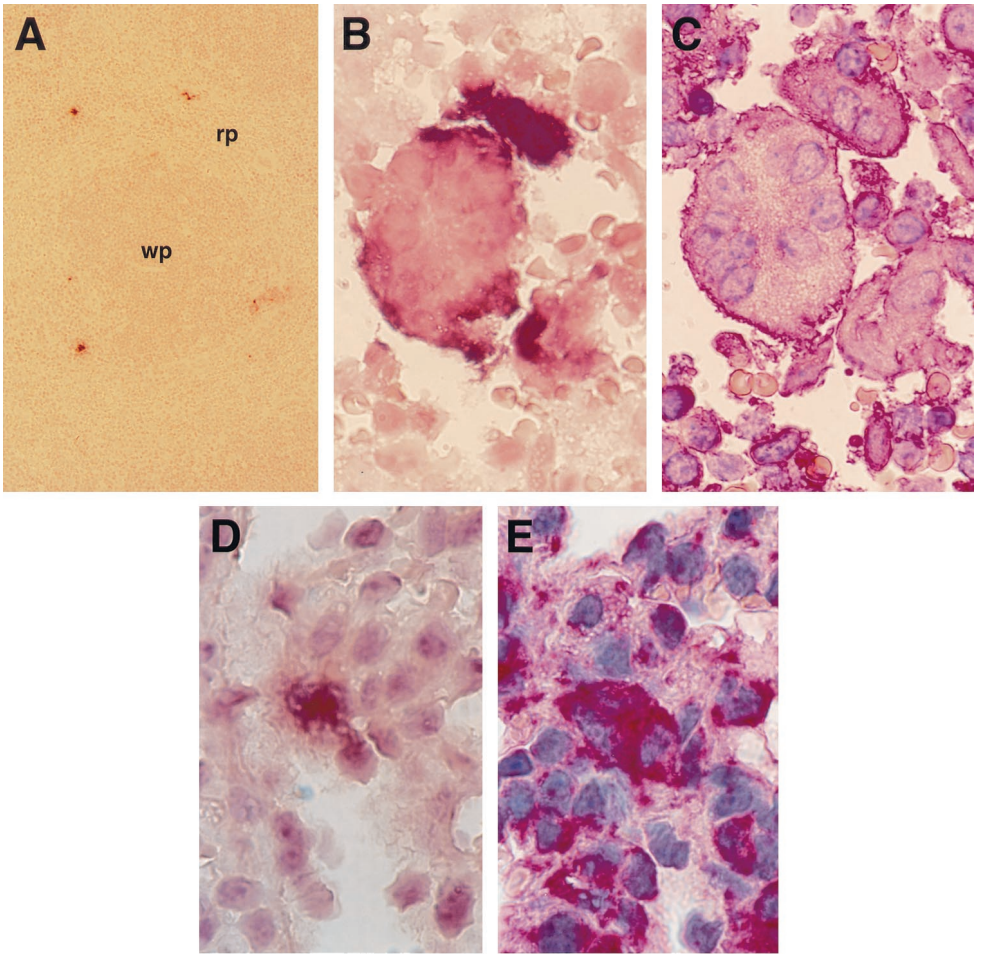

FIG. 1. MV-Ed infects F4/80$^+$ macrophages in spleen and lung. (A to C) Sections of the spleen 3 days after i.p. infection. (A) Low magnification showing MV N RNA-positive cells in the red pulp (rp). (B and C) Consecutive sections showing colocalization of MV N RNA (B) with the MM marker F4/80 (C) in syncytia. (D and E) Consecutive lung sections 6 days after i.p. infection showing MV-specific RNA signals (D) colocalizing with F4/80-positive cells (E). wp, white pulp (darker area). Magnifications, ×87.5 (A) and ×875 (B to E).

inoculation, we examined lymphatic and other organs of these mice for MV replication at 3, 6 or 12 days after i.p. infection. The most prominent virus-specific pathology was observed at 3 days p.i. in lymphatic tissues; multinucleated giant cells expressing MV N mRNA were detected in the spleen (Fig. 1A and B) and in the lymph nodes (data not shown). In the spleen, sites of virus replication were detected in the red pulp and in the marginal zone (Fig. 1A) and sporadically in the white pulp. The combination of MV ISH and cell-specific IHC on consecutive tissue sections was then utilized to identify infected cells. Macrophage (F4/80, MOMA1, and ERTR9), T-cell (CD3, CD4, and CD8), B-cell (B220), and DC (NLDC145 and CD11c) cell markers were analyzed. Colocalization of positive signals was found mainly in F4/80$^+$ macrophages (Fig. 1B and C), occasionally in MOMA1$^+$ cells, and only in a few CD4$^+$ T cells or DC (data not shown), confirming the placement of most infected cells in the macrophage lineage. By 6 days p.i., the replicating virus was detected in other systemic organs, including lungs (Fig. 1D) and liver, kidney, heart, and pancreas (data not shown), and co-localization of replicating virus in the lungs was again observed in F4/80$^+$ cells (Fig. 1D and E). At 14 days p.i., the tissue pathology was moderate if detectable. Nevertheless, single MV replicating cells were observed in brain, approximately 10% of which were macrophages (data not shown).

We then asked if i.c. inoculation of mice with MV-Ed would result in macrophage infection. Indeed, replicating virus was observed during the first week p.i. not only in single F4/80$^+$ cells (Fig. 2A and B) but also in a multinucleated giant F4/80$^+$ cells localized in the brain ventricles (Fig. 2C and D) or parenchyma (intravascular or perivascular), indicating that these circulating cells are susceptible to virus-induced fusion. Thus, F4/80$^+$ cells are targets for MV not only after i.n. but also after i.p. or i.c. virus administration.

DC disseminate MV infection in macrophage-depleted mice. Having shown that macrophages are associated with MV dissemination in Ifnar^{ko}-CD46Ge mice, we examined whether these cells are necessary for efficient propagation of MV infection in these animals. Clodronate liposomes administered by different routes can specifically deplete macrophages in different organs (41). In order to deplete splenic macrophages, Ifnar^{ko}-CD46Ge mice were injected i.p. with clodronate liposomes. Figure 3 documents by specific IHC the extent of depletion of three splenic macrophage subpopulations: the red pulp F4/80$^+$ (Fig. 3D), metallophilic marginal zone MOMA1$^+$

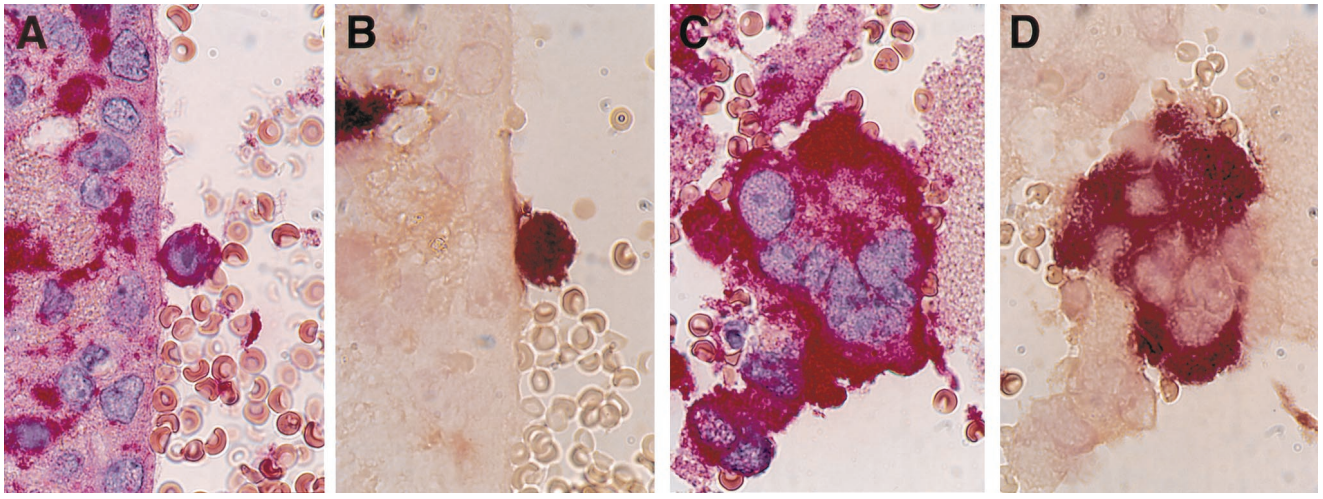

FIG. 2. MV replication in the brain 3 days after i.c. inoculation of mice. Colocalization of F4/80-positive cells (A and C) and MV N mRNA (B and D) within single cells (A and B) and a syncytium (C and D) in the brain ventricle is shown. Magnification, ×875.

(Fig. 3E), and marginal zone ERTR9$^+$ (Fig. 3F) cells. In contrast, control empty-liposome-treated mice showed normal densities and distributions of all macrophages (Fig. 3A, B, and C). In addition, CD11c$^+$ or NLDC145$^+$ DC, 4C11$^+$ follicular DC, and B or T cells were not affected (data not shown). Furthermore, as monitored by the flow cytometric assay, in 10 of 12 mice the clodronate liposomes were effective in eliminating 95% of circulating blood F4/80$^+$ cells, whereas in the two remaining animals approximately 70% depletion was observed (data not shown). Macrophage depletion was observed in livers from clodronate liposome-treated mice but not in their lungs (data not shown). Thus, i.p. injection of Ifnar^{ko}-CD46Ge mice with clodronate liposomes resulted in selective depletion of splenic and liver macrophage subpopulations without any effect on other cell populations, as previously reported for wild-type mice (35).

Three days after clodronate liposomes treatment, the mice were infected with MV-Ed i.p., and at 3 days p.i. blood cells and tissues, including spleen, liver, and lung, were collected and analyzed by MV-specific ISH and cell-specific IHC. MV pathogenesis characterized by viral replication in the white pulp (Fig. 4A), syncytium formation, and apoptosis (pycnotic nuclei in the syncytia shown in Fig. 4B) was observed. MV infection of remaining F4/80$^+$ cells in the red pulp was observed in only a few locations. IHC of tissue sections detected reticular CD11c$^+$ (Fig. 4B) and interdigitating NLDC145$^+$

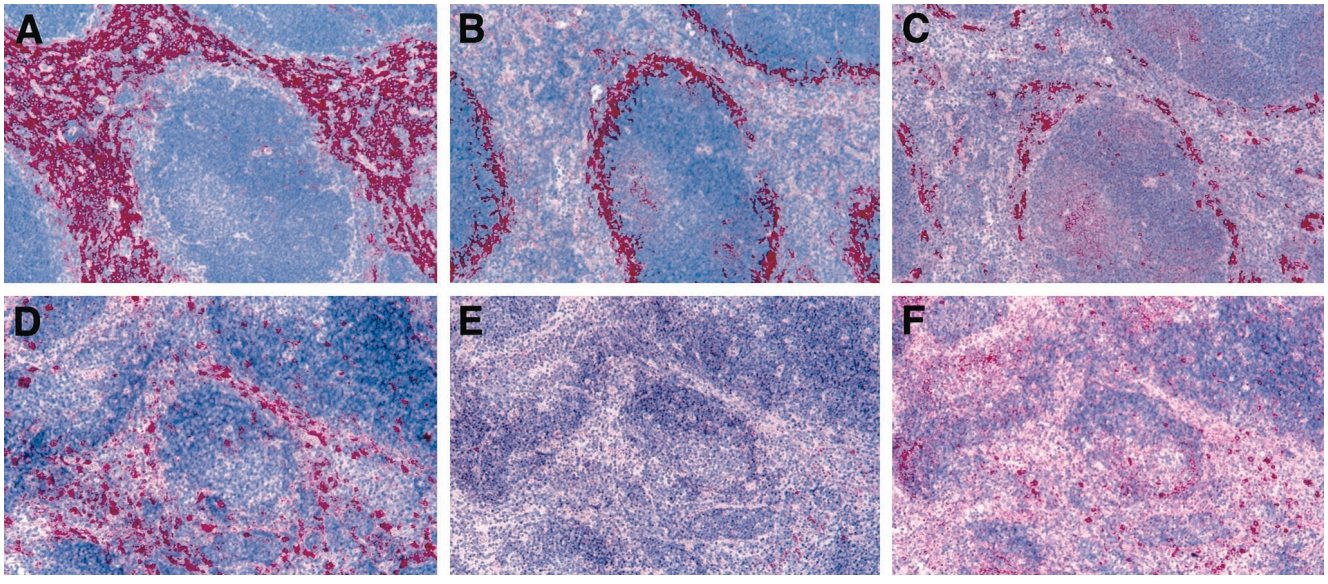

FIG. 3. Depletion of splenic macrophage subpopulations after i.p. treatment with clodronate liposomes. Splenic tissues obtained from mice injected with empty liposomes (A to C) or with clodronate liposomes (D to F) are shown. Six days after treatment, sections were IHC stained for red pulp F4/80$^+$ macrophages (A and D), marginal zone metallophilic MOMA1$^+$ macrophages (B and E), and marginal zone ERTR9$^+$ macrophages (C and F). Magnification, ×77.5.

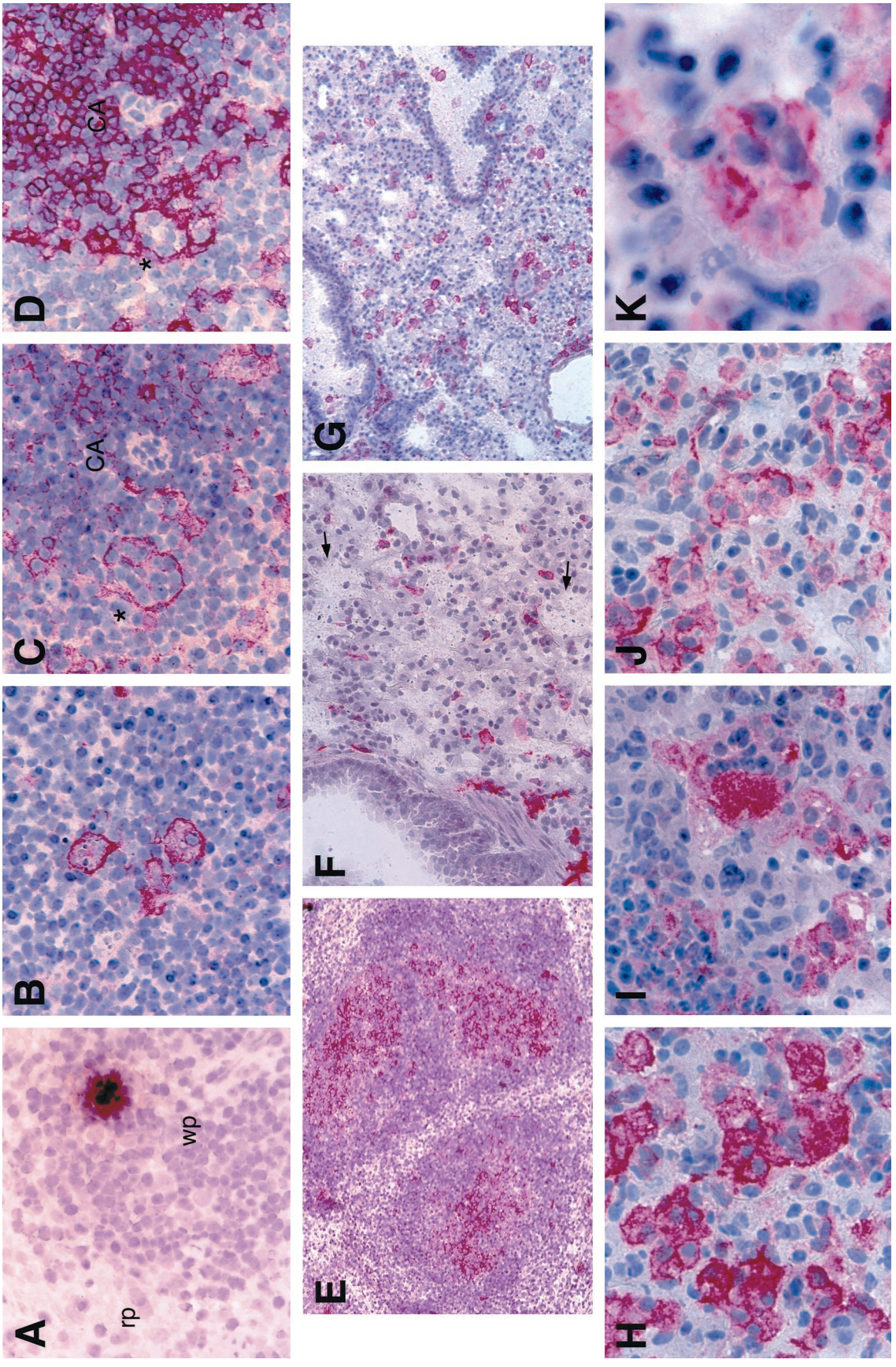

FIG. 4. MV replication and pathogenesis in macrophage-depleted mouse tissues. (A to E) Histological analysis of macrophage-depleted spleens 3 days after i.p. infection with MV-Ed. (A) Area in the white pulp positive for MV N mRNA, rp, red pulp; wp, white pulp. (B) Syncytia stained with the CD11c cell marker. (C and D) Colocalization of the NLDC145 cell marker (C) with a CD4 T-cell marker (D) within a syncytium (asterisk) located in the central periarterial sheath, CA, central artery. (E) Newly formed PNA-positive germinal centers (red) observed at 3 days p.i. within the white pulp. (F to K) Lung pathology after i.n. administration of clodronate liposomes and MV-Ed. (F) Local depletion of F4/80$^+$ macrophages (arrows indicate apoptotic cells). (G) Extensive infiltration of CD11c$^+$ DC in the same tissue block. (H to K) Development of MV-induced syncytia that contain either CD11c$^+$ (H) and NLDC145$^+$ (I) DC or F4/80$^+$ (J) and MOMA1$^+$ (K) macrophages. Magnifications, ×405 (A to D, H, and J); ×101 (E to G); and ×1,013 (K).

TABLE 2. MV N RNA in macrophage-depleted versus intact mouse spleens[a]

Treatment	Days p.i.	No. of mice	Mean (SD) MV N RNA copies/μg of total RNA
Clodronate liposomes	3	10	2×10^7 (5.4×10^6)
	14	6	3×10^6 (5.1×10^5)
Empty liposomes	3	5	2.7×10^6 (8.4×10^5)
	14	2	1×10^6 (both mice)

[a] Mice were injected with clodronate liposomes i.p. and 3 days later were infected with MV-Ed i.p. At 3 or 14 days p.i. spleens were collected, total RNA was isolated, and the viral RNA was quantified as described in Materials and Methods.

(Fig. 4C) DC as the most common cells within syncytia located in the margin of the T- and B-cell areas and in the newly formed germinal center areas of the white pulp. Double-positive $CD3^+$ $CD4^+$ T cells (Fig. 4D) were detected within those $NLDC145^+$ $CD11c^+$ syncytia less frequently, and $CD3^+$ $CD8^+$ T cells or $B200^+$ B cells were detected only occasionally (data not shown).

In addition, the splenic tissue organization revealed very prominent induction of PNA-positive germinal center formation within the majority of splenic follicles (Fig. 4E). Moreover, we detected increased populations of $4C11^+$ follicular DC, many of which were also fused and colocalized with $NLDC145^+$ $CD11c^+$ syncytia within B-cell areas (data not shown). These data suggest that in spleens of macrophage-depleted mice, the main MV replicating cells are $NLDC145^+$ $CD11c^+$ DC located in the white pulp.

To determine if macrophage depletion influenced the viral load in other PBMC, MV H protein expression was analyzed in 10 clodronate liposome-treated $Ifnar^{ko}$-CD46Ge mice in which 95% of circulating blood $F4/80^+$ cells were depleted. Four of these mice expressed H protein on $B220^+$ cells (mean, 0.46%), and two mice expressed H protein on $CD4^+$ cells (mean, 0.66%). H protein was not detectable on the remaining $F4/80^+$ cells; in only two mice with a 70% depletion was H protein detected on these cells. A control mouse treated with empty liposomes had slightly higher expression levels, similar to those of the animals presented in Table 1, second column.

To monitor the effects of macrophage depletion on viral load, total RNA was isolated at 3 days p.i. from the spleens of the same clodronate liposome-treated and control mice. MV N gene transcripts were quantified by RT–real-time PCR by comparison to a standard curve. As shown in Table 2, about 10 times more MV transcripts were detected in total spleen RNA of clodronate liposome-treated mice than in spleens of control mice (2×10^7 versus 2×10^6 molecules/μg of total RNA, corresponding to about 100 versus 10 copies of MV N RNA per cell, respectively). At a later time point (14 days p.i.), the virus load declined in both clodronate liposome-treated and control mice (Table 2). Thus, even if slightly fewer circulating MV-infected PBMC were detected in clodronate liposome-treated mice, MV infection propagated more efficiently in the spleens of these mice than in control mice.

Having observed that the depletion of splenic macrophages resulted in higher levels of DC infection in the spleen, we then sought to verify the effects of the depletion of lung macrophages on MV propagation. To attempt depleting lung macrophages, we treated seven mice i.n. with clodronate liposomes. IHC analysis of lungs revealed nonhomogenous depletion of $F4/80^+$ or $MOMA1^+$ macrophages; areas of lung lobes proximal to the bronchi were more efficiently depleted (Fig. 4F; arrows point to apoptotic cells) than the more distal areas (Fig. 4J and K). However, at 3 days after i.n. MV administration, in such macrophage-depleted lungs a marked infiltration of $CD11c^+$ cells within and below the airway epithelium, and within the alveolar septal walls was found (Fig. 4G). MV was detected in numerous CD11c-positive syncytia (Fig. 4H), many of which were also positive for the NLDC145 cell marker (Fig. 4I). In addition, a weak B-cell infiltration was noted, but there was no effect on T-cell populations (data not shown). Nevertheless, in the same lung sections many infected $F4/80^+$ (Fig. 4J) and $MOMA1^+$ (Fig. 4K) syncytia were also detected, indicating a heterogenous cellular tropism of the virus. The lung pathology after control i.n. administration of empty liposomes followed by MV infection is characterized by high levels of virus replication in $F4/80^+$ syncytia without significant effect on DC, as described for nontreated mouse lungs (27). These observations suggest that in vivo depletion of endogenous lung tissue macrophages resulted in strong local infiltration of DC and in virus infection of both infiltrating $NLDC145^+$ and $CD11c^+$ DC and macrophages.

DISCUSSION

We report here that MV replicates in PBMC, including both MM and lymphoid B or T cells, in two mouse strains expressing CD46 with human-like tissue specificity and efficiency. In particular, MV replication is most prominent in $F4/80^+$ cells shortly after inoculation by three different routes. Thus, it seems plausible that MM serve as early vectors for MV dissemination. When MM were depleted by clodronate liposome treatment, numerous infected DC were detected in the spleen and lungs, and the splenic virus load was increased. Thus, MM support virus replication early after host infection, but they also contribute to protecting other immune cells from infection.

Circulating MM serve as vectors for MV dissemination. Based on the observation that MV-positive $F4/80^+$ cells were often detected in infected organs after i.n. inoculation of $Ifnar^{ko}$-CD46Ge mice, MM were considered as candidate vectors for MV dissemination (27). To further investigate this possibility, we determined if $F4/80^+$ cells could be detected early after infection of $Ifnar^{ko}$-CD46Ge mice not only by the i.n. route but also by the i.p. and i.c. routes. Indeed, 3 days after i.n. inoculation of these mice, about 1.8% of the circulating MM were infected. The percentage of infected MM was above 3% after i.p. infection and was three to four times higher than that of infected B- and CD4-positive T cells. These results are consistent with efficient virus uptake and replication by macrophages, which are numerous in the peritoneum. The third inoculation route was i.c., resulting again in efficient infection of $F4/80^+$ cells. Thus, macrophages are consistently and rapidly infected after MV inoculation. This is the case not only for $Ifnar^{ko}$-CD46Ge mice but also for the parental line CD46Ge, where about 1.4% of circulating $F4/80^+$ macrophages were infected shortly after i.p. inoculation. However, these animals were able to rapidly clear the infection, while in $Ifnar^{ko}$-CD46Ge mice MV infection disseminated systemically.

Quantitative data regarding the percentages of different subspecies of PBMC infected during acute measles are not available, but 0.01 to 2% of total PBMC were productively MV infected 2 to 3 days after onset of the rash in adults with severe acute measles (10). Moreover, data on the percentage of MV-infected cells after i.c. inoculation of neonatal CD46-expressing mice, collection of their spleens, and analysis of separated splenocytes have been obtained (31). In different populations of splenocytes, including CD8-positive cells, 0.09 to 1.0% MV-infected cells were observed. Thus, even at the peak of severe acute measles in humans and of experimental infection of mice, only a small fraction of immune cells appear to productively replicate MV.

Can infections of CD46-expressing mice be expected to faithfully mimic acute MV infection in humans? More than one receptor is involved in MV entry in human cells (39), and late events in MV replication are restricted in certain mouse cells (42). Therefore, it may not be realistic to expect faithful reproduction of all aspects of human MV infections in transgenic mice. Nevertheless, the data presented here do suggest that MV infection of PBMC in CD46-expressing mice may mimic several aspects of PBMC infection in acute measles in humans.

MM depletion results in more efficient DC infection. To further characterize their role as host cells in MV infections of mice, macrophages were selectively depleted by treatment with clodronate liposomes (41), a method previously used to study other viral infections (16, 35). After i.p. administration of clodronate liposomes, we observed in Ifnar^{ko}-CD46Ge mice the depletion of circulating F4/80$^+$ MM and of three different splenic macrophage populations: red pulp F4/80$^+$, metallophilic marginal zone MOMA1$^+$, and marginal zone ERTR9$^+$ macrophages. The other splenic cells, including DC and nonphagocytic lymphoid B or T cells, were not affected, consistent with data obtained for other mouse strains showing that apart from macrophages, only their direct monocytic precursors are depleted by clodronate liposomes treatment (19, 35).

In such macrophage-depleted mice infected i.p. with MV, virus replication in splenic tissues differed in microanatomical location and infected cell types compared to that in control mice expressing normal macrophage levels. In control mice, MV replication was located in the red pulp and the marginal zone, primarily in fused F4/80$^+$ or MOMA1$^+$ macrophages. CD3$^+$ CD4$^+$ T cells were rarely detected within the syncytia, and DC were detected only in a few syncytia located in the white pulp. Previously, in mice infected i.n. with MV a low level of infected thymic NLDC145$^+$ CD11c$^+$ DC was observed during the late phase of infection (27). In contrast, in macrophage-depleted mice MV replicated mainly in the white pulp, and numerous fused NLDC145$^+$ CD11c$^+$ DC were observed. Moreover, at the interface between T- and B-cell areas, CD4$^+$ CD3$^+$ T cells were involved in syncytia that were also positive for NLDC145$^+$ CD11c$^+$ cells. Finally, in B-cell areas and in newly formed germinal centers, B220$^+$ cells or 4C11$^+$ follicular DC were involved in syncytia. These data from spleens and similar observations for lungs strongly suggest that infected DC may fuse to local neighboring immune cells. Thus, in untreated mice macrophages may protect DC from MV infection.

It is noted that in clodronate liposome-treated mice the splenic viral load increased by about 10 times at 3 days p.i., which is a small factor compared to increases observed in macrophage-depleted mice infected with two other macrophage-tropic viruses, namely, murine cytomegalovirus and lymphocytic choriomeningitis virus (16, 35). This increase in viral load is consistent with the observation that the interaction of MV-infected DC with T cells in vitro induces syncytium formation where MV undergoes more efficient replication than in MV-infected monocytes (11). It is conceivable that DC infection might have other effects on MV pathogenesis, especially on the induction of host immunity. In particular, the induction of germinal center formation is rapid and occurs already at 3 days p.i., much earlier than by day 12 as after other viral infections. Germinal centers are required to maintain high-level production of neutralizing antibodies (2).

Innate immunity and dissemination of MV infection. It is interesting that prominent infiltration with and activation of immune cells, including those with DC-like morphology, was also described after in vivo depletion of alveolar macrophages of wild-type mice (40) or in pulmonary tissues of rats (18) treated with a nonviral antigen. To explain these findings, it was suggested that the uptake of pathogens primarily by macrophages may contribute to a fine-tuned balance that must provide not only protection from the pathogen but also limitation of excessive tissue destruction which can be induced by a strong host immune reaction.

This might also be valid for MV infections. The innate immune system consisting of endogenous macrophages and freshly recruited monocytes may be responsible for the early capture and dissemination of MV in Ifnar^{ko}-CD46Ge mice. After experimental depletion of endogenous macrophages, DC residing in local tissues (3) may more readily capture MV and be activated. Those DC that have internalized and are replicating the virus, or that have absorbed it on their surface (12), may then leave the local tissues and migrate into the white pulp of the spleen where they stimulate the effector T and B cells of the adaptive immune system. By doing so, DC may also disseminate the infection throughout the host tissues and subsequently seed neighboring permissive cells, similar to the case for human immunodeficiency virus (6, 12).

It is important to determine the consequences for the immune response of the switch of MV dissemination from MM to DC. It is conceivable that enhanced DC infection may result in immune suppression due to the apoptosis of DC and of the contacted T cells (11). In an opposite scenario, enhanced presentation of MV antigens by DC may lead to more prominent induction of both antiviral neutralizing B-cell immunity and T-cell-mediated immunity (22, 23). The rapid induction of germinal centers appears to be consistent with this scenario. If antiviral immunity is stronger after enhanced DC infection, recombinant MV targeting DC may be more efficient vaccines.

ACKNOWLEDGMENTS

This work was supported by grant 31-45900.95 of the Schweizerischer Nationalfonds to R.C. and by the Siebens and Mayo Foundations. The salary of Branka Roscic-Mrkic was provided in part by grant 3786.1 of the Commission for Technology and Innovation and grant 31-43475.95 of the Schweizerischer Nationalfonds to M.A.B.

We thank Marianne König and Lenka Vlk for technical assistance, Fritz Ochsenbein for graphic work, and Eric Poeschla for comments on the manuscript.

REFERENCES

1. **Albrecht, P., D. Lorenz, M. J. Klutch, J. H. Vickers, and F. A. Ennis.** 1980. Fatal measles infection in marmosets: pathogenesis and prophylaxis. Infect. Immun. **27:**969–978.
2. **Bachmann, M. F., B. Odermatt, H. Hengartner, and R. M. Zinkernagel.** 1996. Induction of long-lived germinal centers associated with persisting antigen after viral infection. J. Exp. Med. **183:**2259–2269.
3. **Banchereau, J., and R. M. Steinman.** 1998. Dendritic cells and the control of immunity. Nature **392:**245–252.
4. **Blixenkrone-Moller, M., A. Bernard, A. Bencsik, N. Sixt, L. E. Diamond, J. S. Logan, and T. F. Wild.** 1998. Role of CD46 in measles virus infection in CD46 transgenic mice. Virology **249:**238–248.
5. **Borrow, P., and M. B. A. Oldstone.** 1995. Measles virus-mononuclear cell interactions. Curr. Top. Microbiol. Immunol. **191:**85–100.
6. **Cameron, P. U., P. S. Freudenthal, J. M. Barker, S. Gezelter, K. Inaba, and R. M. Steinman.** 1992. Dendritic cells exposed to human immunodeficiency virus type-1 transmit a vigorous cytopathic infection to CD4+ T cells. Science **257:**383–387.
7. **Dörig, R. E., A. Marcil, A. Chopra, and C. D. Richardson.** 1993. The human CD46 molecule is a receptor for measles virus (Edmonston strain). Cell **75:**295–305.
8. **Esolen, L. M., B. J. Ward, T. R. Moench, and D. E. Griffin.** 1993. Infection of monocytes during measles. J. Infect. Dis. **168:**47–52.
9. **Fearon, D. T., and R. M. Locksley.** 1996. The instructive role of innate immunity in the acquired immune response. Science **272:**50–53.
10. **Forthal, D. N., S. Aarnaes, J. Blanding, L. de la Maza, and J. G. Tilles.** 1992. Degree and length of viremia in adults with measles. J. Infect. Dis. **166:**421–424.
11. **Fugier-Vivier, I., C. Servet-Delprat, P. Rivailler, M. C. Rissoan, Y. J. Liu, and C. Rabourdin-Combe.** 1997. Measles virus suppresses cell-mediated immunity by interfering with the survival and functions of dendritic and T cells. J. Exp. Med. **186:**813–823.
12. **Geijtenbeek, T. B., D. S. Kwon, R. Torensma, S. J. van Vliet, G. C. van Duijnhoven, J. Middel, I. L. Cornelissen, H. S. Nottet, V. N. KewalRamani, D. R. Littman, C. G. Figdor, and Y. van Kooyk.** 2000. DC-SIGN, a dendritic cell-specific HIV-1-binding protein that enhances trans-infection of T cells. Cell **100:**587–597.
13. **Griffin, D. E., and W. J. Bellini.** 1996. Measles virus, p. 1267–1312. *In* B. N. Fields, D. M. Knipe, P. M. Howley, et al. (ed.), Fields virology, 3rd ed. Lippincott-Raven Publishers, Philadelphia, Pa.
14. **Grosjean, I., C. Caux, C. Bella, I. Berger, F. Wild, J. Banchereau, and D. Kaiserlian.** 1997. Measles virus infects human dendritic cells and blocks their allostimulatory properties for CD4+ T cells. J. Exp. Med. **186:**801–812.
15. **Hall, W. C., R. M. Kovatch, P. H. Herman, and J. G. Fox.** 1971. Pathology of measles in rhesus monkeys. Vet. Pathol. **8:**309–319.
16. **Hanson, L. K., J. S. Slater, Z. Karabekian, H. W. Virgin IV, C. A. Biron, M. C. Ruzek, N. van Rooijen, R. P. Ciavarra, R. M. Stenberg, and A. E. Campbell.** 1999. Replication of murine cytomegalovirus in differentiated macrophages as a determinant of viral pathogenesis. J. Virol. **73:**5970–5980.
17. **Helin, E., A. A. Salmi, R. Vanharanta, and R. Vainionpaa.** 1999. Measles virus replication in cells of myelomonocytic lineage is dependent on cellular differentiation stage. Virology **253:**35–42.
18. **Holt, P. G., J. Oliver, N. Bilyk, C. McMenamin, P. G. McMenamin, G. Kraal, and T. Thepen.** 1993. Downregulation of the antigen presenting cell function(s) of pulmonary dendritic cells in vivo by resident alveolar macrophages. J. Exp. Med. **177:**397–407.
19. **Huitinga, I., J. G. Damoiseaux, N. van Rooijen, E. A. Dopp, and C. D. Dijkstra.** 1992. Liposome mediated affection of monocytes. Immunobiology **185:**11–19.
20. **Karp, C. L., M. Wysocka, L. M. Wahl, J. M. Ahearn, P. J. Cuomo, B. Sherry, G. Trinchieri, and D. E. Griffin.** 1996. Mechanism of suppression of cell-mediated immunity by measles virus. Science **273:**228–231.
21. **Kemper, C., M. Leung, C. B. Stephensen, C. Pinkert, M. K. Liszewski, R. Cattaneo, and J. P. Atkinson.** Membrane cofactor protein (CD46:MCP) transgenic mice. Clin. Exp. Immunol., in press.
22. **Ludewig, B., K. J. Maloy, C. Lopez-Macias, B. Odermatt, H. Hengartner, and R. M. Zinkernagel.** 2000. Induction of optimal anti-viral neutralizing B cell responses by dendritic cells requires transport and release of virus particles in secondary lymphoid organs. Eur. J. Immunol. **30:**185–196.
23. **Ludewig, B., S. Oehen, F. Barchiesi, R. A. Schwendener, H. Hengartner, and R. M. Zinkernagel.** 1999. Protective antiviral cytotoxic T cell memory is most efficiently maintained by restimulation via dendritic cells. J. Immunol. **163:** 1839–1844.
24. **McChesney, M. B., C. J. Miller, P. A. Rota, Y. D. Zhu, L. Antipa, N. W. Lerche, R. Ahmed, and W. J. Bellini.** 1997. Experimental measles. I. Pathogenesis in the normal and the immunized host. Virology **233:**74–84.
25. **Mesquita, R., E. Castanos-Velez, P. Biberfeld, R. M. Troian, and M. M. De Siqueira.** 1998. Measles virus antigen in macrophage/microglial cells and astrocytes of subacute sclerosing panencephalitis. APMIS **106:**553–561.
26. **Moench, T. R., D. E. Griffin, C. R. Obriecht, A. J. Vaisberg, and R. T. Johnson.** 1988. Acute measles in patients with and without neurological involvement: distribution of measles virus antigen and RNA. J. Infect. Dis. **158:**433–442.
27. **Mrkic, B., B. Odermatt, M. A. Klein, M. A. Billeter, J. Pavlovic, and R. Cattaneo.** 2000. Lymphatic dissemination and comparative pathology of recombinant measles viruses in genetically modified mice. J. Virol. **74:**1364–1372.
28. **Mrkic, B., J. Pavlovic, T. Rulicke, P. Volpe, C. J. Buchholz, D. Hourcade, J. P. Atkinson, A. Aguzzi, and R. Cattaneo.** 1998. Measles virus spread and pathogenesis in genetically modified mice. J. Virol. **72:**7420–7427.
29. **Nakayama, T., T. Mori, S. Yamaguchi, S. Sonoda, S. Asamura, R. Yamashita, Y. Takeuchi, and T. Urano.** 1995. Detection of measles virus genome directly from clinical samples by reverse transcriptase-polymerase chain reaction and genetic variability. Virus Res. **35:**1–16.
30. **Naniche, D., G. Varior-Krishnan, F. Cervoni, T. F. Wild, B. Rossi, C. Rabourdin-Combe, and D. Gerlier.** 1993. Human membrane cofactor protein (CD46) acts as a cellular receptor for measles virus. J. Virol. **67:**6025–6032.
31. **Oldstone, M. B., H. Lewicki, D. Thomas, A. Tishon, S. Dales, J. Patterson, M. Manchester, D. Homann, D. Naniche, and A. Holz.** 1999. Measles virus infection in a transgenic model: virus-induced immunosuppression and central nervous system disease. Cell **98:**629–640.
32. **Polack, F. P., P. G. Auwaerter, S. H. Lee, H. C. Nousari, A. Valsamakis, K. M. Leiferman, A. Diwan, R. J. Adams, and D. E. Griffin.** 1999. Production of atypical measles in rhesus macaques: evidence for disease mediated by immune complex formation and eosinophils in the presence of fusion-inhibiting antibody. Nat. Med. **5:**629–634.
33. **Radecke, F., P. Spielhofer, H. Schneider, K. Kaelin, M. Huber, C. Dotsch, G. Christiansen, and M. A. Billeter.** 1995. Rescue of measles viruses from cloned DNA. EMBO J. **14:**5773–5784.
34. **Schnorr, J. J., S. Xanthakos, P. Keikavoussi, E. Kampgen, V. ter Meulen, and S. Schneider-Schaulies.** 1997. Induction of maturation of human blood dendritic cell precursors by measles virus is associated with immunosuppression. Proc. Natl. Acad. Sci. USA. **94:**5326–5331.
35. **Seiler, P., P. Aichele, B. Odermatt, H. Hengartner, R. M. Zinkernagel, and R. A. Schwendener.** 1997. Crucial role of marginal zone macrophages and marginal zone metallophils in the clearance of lymphocytic choriomeningitis virus infection. Eur. J. Immunol. **27:**2626–2633.
36. **Sergiev, P. G., N. E. Ryazantseva, and I. G. Shroit.** 1960. The dynamics of pathological processes in experimental measles in monkeys. Acta Virol. **4:**265–273.
37. **Sherman, F. E., and R. G.** 1958. In vivo and in vitro cellular changes specific for measles. AMA Arch. Pathol. **65:**587–599.
38. **Stryker, W. A.** 1940. Disseminated giant cell reaction: a possible prodrome of measles. Am. J. Dis. Child. **59:**468–478.
39. **Tatsuo, H., N. Ono, K. Tanaka, and Y. Yanagi.** 2000. SLAM (CDw150) is a cellular receptor for measles virus. Nature **406:**893–897.
40. **Thepen, T., N. Van Rooijen, and G. Kraal.** 1989. Alveolar macrophage elimination in vivo is associated with an increase in pulmonary immune response in mice. J. Exp. Med. **170:**499–509.
41. **Van Rooijen, N., and A. Sanders.** 1994. Liposome mediated depletion of macrophages: mechanism of action, preparation of liposomes and applications. J. Immunol. Methods **174:**83–93.
42. **Vincent, S., D. Spehner, S. Manie, R. Delorme, R. Drillien, and D. Gerlier.** 1999. Inefficient measles virus budding in murine L.CD46 fibroblasts. Virology **265:**185–195.
43. **White, R. G., and J. F. Boyd.** 1973. The effect of measles on the thymus and other lymphoid tissues. Clin. Exp. Immunol. **13:**343–357.
44. **Yannoutsos, N., J. N. Ijzermans, C. Harkes, F. Bonthuis, C. Y. Zhou, D. White, R. L. Marquet, and F. Grosveld.** 1996. A membrane cofactor protein transgenic mouse model for the study of discordant xenograft rejection. Genes Cells **1:**409–419.
45. **Zhu, Y. D., J. Heath, J. Collins, T. Greene, L. Antipa, P. Rota, W. Bellini, and M. McChesney.** 1997. Experimental measles. II. Infection and immunity in the rhesus macaque. Virology **233:**85–92.